FINITE ELEMENT MODELLING OF REINFORCED CONCRETE SLAB EXPOSED TO EXTREME FIRE LOADS

Daniel JINDRA[1], *Petr HRADIL*[1]

[1]Institute of Structural Mechanics, Faculty of Civil Engineering, Brno University of Technology, Veveří 331/95, 602 00 Brno, Czech Republic

jindra.d@fce.vutbr.cz, hradil.p@fce.vutbr.cz

DOI: 10.35181/tces-2019-0012

Abstract. *Numerical approach using the finite element method has been used to determine the mechanical resistance (criterion R) of a reinforced concrete structure exposed to fire. Geometry of the structure is considered as a simply supported slab in one dimension. Fire load has been defined by a nominal standard ISO 834 fire curve. Both, thermal and structural response are obtained using a finite element method software ANSYS. Temperature-dependent nonlinear thermal and mechanical properties of concrete and reinforcement are adopted in accordance with Eurocode standards. Nonlinear material model Menetrey-Willam with exponential functions for compression hardening (and softening) and tension softening has been used to describe the behaviour of concrete elements. Discrete option of modelling reinforcement has been considered. Mechanical resistance of the slab is determined by reaching the limit mid-span deformation. Results have been compared with simplified method of isotherm 500 °C described in Eurocode.*

Keywords

Extreme loads, mechanical fire resistance, Menetrey-Willam material model, numerical nonlinear analysis, reinforced slab structure, transient fire response.

1. Introduction

Numerical approach in determining the resistance of reinforced concrete structures exposed to fire has been recently increasing with the development of FEM software. Commercially available software ANSYS has the capability to perform nonlinear calculations, thermal as well as mechanical. Some examples are possible to be studied under these references: [1], [2], [3], [4], [5], [6], [7] and [8]. Usually different material models for concrete structures have been used. In this study, recently implemented material model in ANSYS [9], nonlinear Menetrey-Willam material model developed by Dynardo GmbH [10] is examined.

In this paper, the first level of complexity and size of a structure according to [11] is analysed. Therefore, it is possible to compare the results of analysis with expected results according to the simplified method of isotherm 500 °C described in [11].

Although a plane strain structure is being analysed, due to more realistic assessment of steel reinforcement in a cross-section of the slab, a 3D model is developed. Finite element model consists of solid elements representing concrete. To provide extra discrete reinforcement to certain concrete elements, special type of reinforcing elements has been applied inside these 3D solid elements referred as base elements.

2. Calculation Methodology

The analysis is carried out using FEM software ANSYS, Classic APDL environment. Coupled-field 3D elements SOLID226 [9] with thermal and translational degrees of freedom to model both, thermal and structural analysis exist, but does not support suitable non-linear material models for concrete. In case of high temperature loads while the structure is exposed to fire, non-linear analysis is recommended. To model suitable non-linear concrete behaviour, 3D elements SOLID65 has been widely used [4], [5] and [8]. Instead this legacy element [9], a current technology SOLID185 with full integration method has been used, as recommended [9]. These elements have only translational degrees of freedom and does not support coupled-field analysis.

The first calculation step in fire resistance analysis of the structure is to determine the thermal response in the form of time-dependent temperature distribution. After this transient thermal analysis throughout the structure for the entire duration of the fire has been carried out, full transient structural analysis is performed. Temperatures from the previous transient thermal analysis are applied as body force nodal loads in the structural analysis.

In transient thermal analysis, fire load has been defined as a convection and radiation as described in [12]. Ambient

air temperatures have been defined by the nominal standard ISO 834 fire curve, which is monotonically increasing function of ambient air (gases) temperatures in time.

Objective of the structural analysis is to compare the mechanical resistance of the slab determined by reaching the limit mid-span deformation [13] with expected results calculated according to the simplified method of isotherm 500 °C [11]. For the simply supported RC slabs of certain geometries, load-bearing capacities of the cross-sections in a simple bending have been estimated for each of 6 classes of mechanical resistances (criterion R) while exposed to fire: ranging from R30 to R240. For each analysis, these loads have been applied as evenly distributed static surface loads at the upper surface of the slab before the application of the temperature loads during the transient analysis. The approach described above is considered as default, chronologically correct, marked with index "#1". In this approach, the mechanical resistance of the slab is described as the time (duration of the standardized fire) of reaching the limit mid-span deformation.

In case of the second approach marked with index "#2", the expected [11] structural surface load is being applied simultaneously with the nodal temperature loads during the transient structural analysis. Estimated structural load is for each case applied linearly with increasing time, starting with the initiation of the fire load and ending at the time of currently examined fire resistance class R. Therefore, the load speed is different for each case, increasing towards lower classes of the resistance R (larger load to be applied during the lesser time). In this approach, only the self-weight of the structure is truly applied as a static load, before the transient loads. The influence of the structural loading speed on the dynamic effects during the transient analysis is negligible, so the loading of the slab could be considered as a static one. After reaching the examined time of the fire resistance class, the structural load is constant in time, and only the nodal temperature loads are increasing. Therefore, in this approach, the mechanical resistance of the slab is also described by the time in the same way as #1, assuming the resistance is reached after all the structural load has been applied.

The approach marked as "#3" is a partial chronological reverse of the case "#1". The self-weight of the structure has been applied in the first step as a static load (same as in #1). In the second step of transient analysis, the nodal temperature loads are increasing until the time of examined fire resistance class R. From this point of time in transient analysis, temperatures of all the nodes remains invariable. At this moment, the mechanical loading is initiated, rising in time by the same speed for all the classes: 10 $kN \cdot m^{-2} \cdot hod^{-1}$. In this approach, the mechanical resistance is described as a limit load value applied when the limit deformation was reached.

In this analysis, the force-lead deformation is being examined, therefore the termination of the analysis is rapidly influenced by the initiation of concrete softening in compression. The mechanical force load is generally only increasing. With a little exception of the self-weight load, where the density of concrete is slightly decreasing in dependence on increasing temperature, also during the structural analysis, what leads to a certain type of unloading of the structure, but this was considered as negligible.

The nodal temperature loads during the transient analysis are also only increasing, therefore the implicit analysis is suitable for this problematic. Explicit model is recommended when the cooling phase of the fire (parametric or real-fire models) is modelled. Therefore, the fact whether the load induced thermal strain (LITS) is incorporated into the model is not significant [14].

3. Finite Element Model

The sequentially coupled thermo-mechanical analysis procedure requires two models with the same geometry to be developed [8]:

- The first is used in transient thermal analysis, to evaluate the thermal response of the structure,
- the second to be used in the transient structural analysis, where mechanical and nodal temperature loads are applied to obtain the physical response of the structure.

3.1. Modelling assumptions

In the development of the numerical model, the following assumptions are made:

- Perfect bond between steel reinforcement and concrete is assumed. This results in the equal total strain in the reinforcement and concrete elements. Bond-slip is not taken into account. Although, an inclusion of the interfacial behaviour leads to more accurate predictions, the effect may be ignored when the objective of the analysis is to obtain the global response of the structure [15].
- Fire induced spalling is not considered in the analysis. Ordinary performance concrete usually resists rapid heating rates with only minor spalling or even without spalling. [16] As a low moisture level is assumed, and the analysis is focused on a normal strength concrete, with higher porosity and permeability than in a high-performance concretes, high pore pressures that might lead to failure due to explosive spalling are avoided [8].
- In both analyses, the mean values of all the material parameters have been used.
- Initial stiffness of the slab is adopted without considering a creep softening of the elastic modulus.

3.2. Thermal Model Development

For the transient thermal analysis, geometry of the slab is discretized using 3D 8-node elements SOLID70, with a single degree of freedom at each node point, temperature. Only elements for concrete are modelled. Application of special reinforcing elements REINF264 inside SOLID70 in this analysis has no effect, as these elements are defined by the same nodes as their base elements, and have only translational or rotational degrees of freedom - same as base elements into which are applied. The orientation of steel reinforcement in longitudinal direction of the slab, therefore perpendicular to the direction of the heat flow, has negligible effect on the heat transfer along the vertical cross section of the slab. In case of stirrups, there might be some noticeable local influence, but concerning the cross-section area, probably negligible as well. In this study however, only slab structures were examined, with no reinforcement parallel to the heat flow during the thermal analysis.

Surface elements SURF152 are added to the bottom surface of the slab (exposed to fire load), to apply thermal load in terms of convection and radiation, as depicted in Fig. 1. Convection film coefficient is set up $\alpha = 25\ W{\cdot}m^{-2}{\cdot}K^{-1}$ for the exposed surface. Emissivity related to the concrete surface is adopted as $\varepsilon = 0.7$. Both these values are considered independent on the temperature. For the unexposed surface, no temperature load and no convection film coefficients have been applied, so the results of the temperature fields in time comply with Appendix [11]. Reference and uniform temperatures are both set up as 20 °C.

The same mesh is used for the thermal and structural model. Although in this case the heat transfer applies only throughout the cross-section in the vertical direction and is constant along the other dimensions, it is more convenient to use the same mesh, so the nodal temperature load could be comfortably applied from the results file of thermal analysis without any adjustments. There is no necessity to save computational time during the thermal analysis in case of coarser mesh.

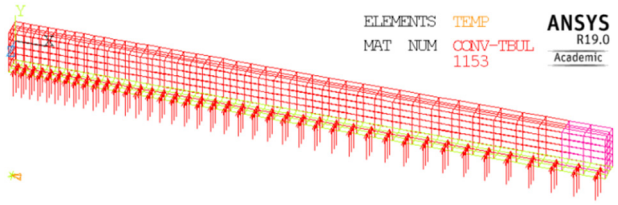

Fig. 1: Finite element mesh for thermal analysis of the slab.

Modelled structure is simply supported slab of height 150 mm with a structural span equal to 4 m. To save computational time during the structural analysis symmetrical boundary conditions have been applied in the mid-span cross section, and only a half of the span is being modelled. Mesh element sizes in the directions of the cross section are adopted as 25 mm. In a longitudinal direction of the slab the length of elements increases from the mid-span (approx. 27 mm) towards the edge supports (approx. 81 mm), as depicted in the Fig. 1.

Values of concrete parameters required to carry out the transient thermal analysis, specific heat capacity c, density ρ and thermal conductivity λ have been adopted in dependence on temperature according to [11]. These parameters do not significantly depend on the strength class of the concrete.

3.3. Structural Model

After transient analysis has been carried out, the thermal elements have been switched to structural ones, SOLID185, with three translational degrees of freedom at each node. Translational boundary constrains in the lateral direction have been applied along the transversal sides of the narrow segment of the slab to model plane strain. Reinforcing elements have been inserted into the picked base elements (see Fig. 2.). The width of modelled narrow segment of the slab is equal to 75 mm. Three options of diameter of the reinforcing bar have been modelled: Ø12, Ø8 and Ø6 mm. In each of the cases, the position of the rebar axis in the cross section is the same, in the distance of 1.5 times of the element size, therefore 37.5 mm. The first variant of slab reinforcing could be then described as: Ø12 a 75 mm, c = 31.5 mm.

Concrete grade C25/30 mixed with siliceous aggregate is considered in the analysis. All the mechanical parameters (also thermal strain) are adopted in dependence on temperature according to [11] and / or [17]. The temperature dependent parameters for Menetrey-Willam material model have been based on the stress-strain curves provided for concrete in [11]. The Menetrey-Willam constitutive model is based on the Willam-Warnke yield surface, incorporating dependence on three independent invariants of the stress tensor [9]. Exponential function for tensional softening of concrete has been adopted, as described in [9].

For steel reinforcement (B550B), a multi-linear material model with isotropic hardening has been defined. The mean value of yield strength at 20 °C has been adopted as 632 MPa. The values of all material parameters have been defined for 20 °C temperature and then in each 100 °C difference for both materials.

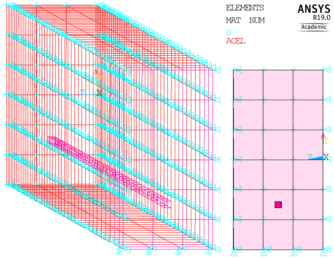

Fig. 2: Finite element mesh of the plane strain 3D model of slab.

Non-linear full transient structural analysis with stepped loading has been carried out. Newmark algorithm has been used for time integration.

4. Response of the Structure

4.1. Thermal Response

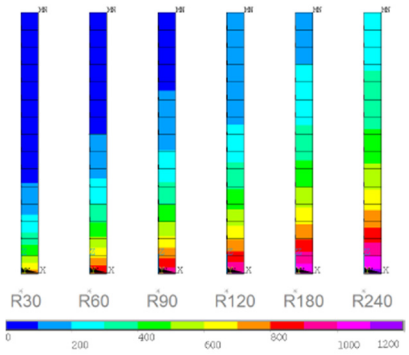

Fig. 3: Temperature profiles of concrete slab of height 150 mm.

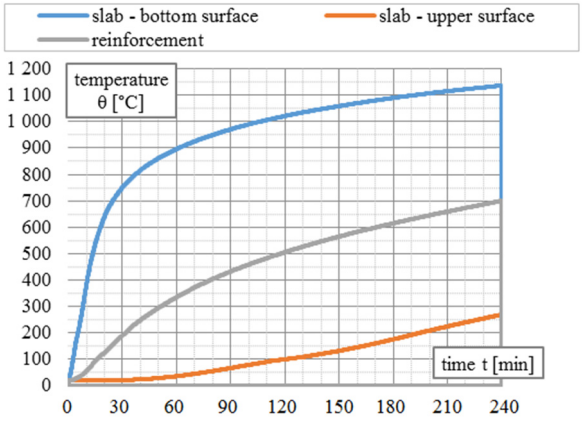

Fig. 4: Temperature evolution in the reinforcement.

Temperature profiles of slab (Fig. 3) have been verified based on Annex A of [11].

Temperature evolution in the reinforcement (Fig. 4) is available when structural response is examined, as there are no reinforcement elements in thermal analysis. Depicted temperature of REINF264 elements is the averaged temperature of base element nodes.

4.2. Structural Response

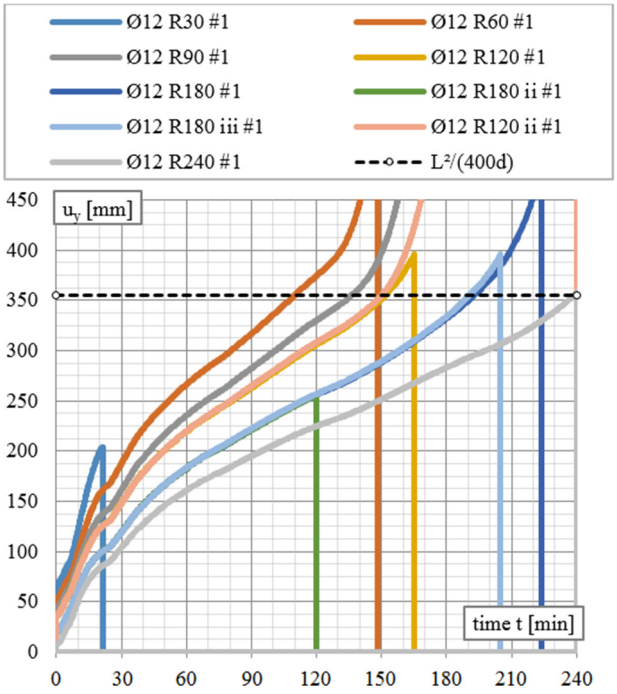

Fig. 5: Evolution of mid-span deformation for geometry Ø12.

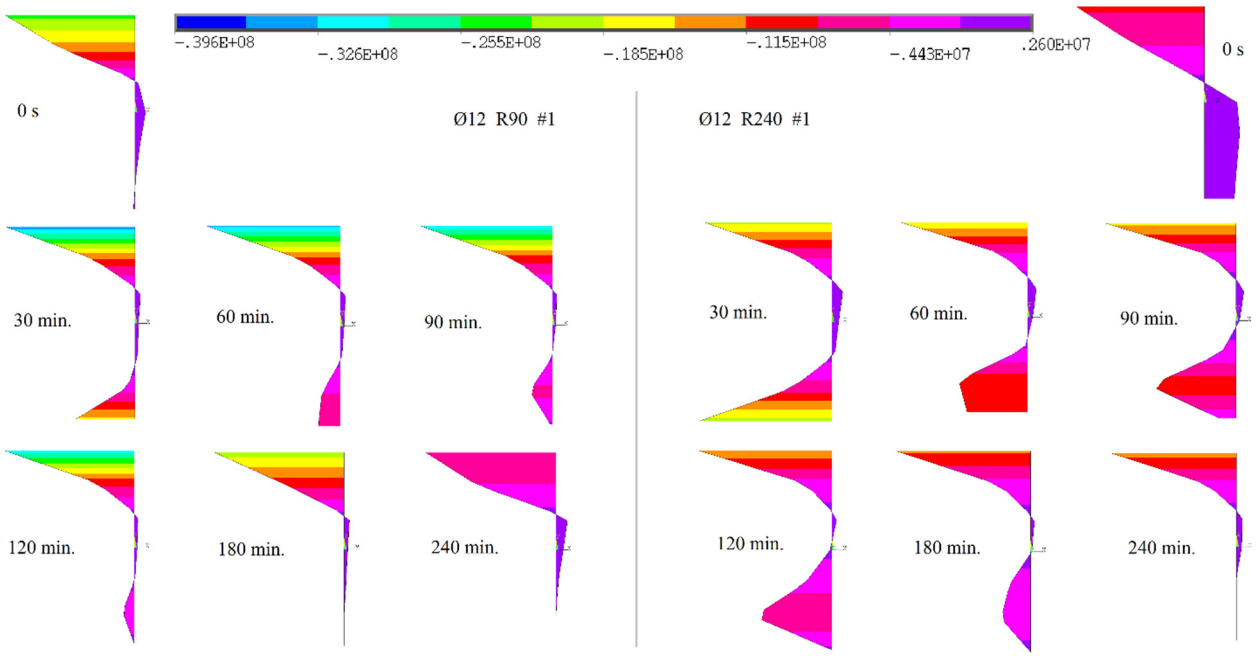

Fig. 6: Normal stress [Pa] in mid-span cross sections of the slab for mechanical resistance criterions R90 (left) and R240 (right) in time.

Time-step increment of transient analysis needs to be decreased (e.g. from 10 s to 2 s) to achieve better convergences while analysing lower classes R of the mechanical response of the structure. In the case of class R30 the expected resistance has not been reached (Fig. 5).

Rising temperatures in concrete introduce thermal strains and degradation of material properties. Thermal expansion and significant decrease of slab stiffness result in increasing deformation of the slab, as presented in Fig. 5, Fig. 7, Fig. 9, Fig. 12 and Fig. 13.

Figure 6 shows the development of normal stress in the mid-span cross section in concrete slab for two classes, R90 and R240 (less mechanical load). Due to large thermal gradient in the first minutes of the fire, significantly large thermal strain is developed on the exposed (bottom) surface of the slab. Although thermal expansion of the heated parts is not constrained by the global boundary conditions in the longitudinal direction, it is indirectly constrained by the significantly higher stiffness of surrounding elements located towards unexposed surface. Therefore, compression is rising in concrete areas exposed to thermal action, similar to analysis [8]. Total strain is given by [9]:

$$\varepsilon_{total} = \varepsilon_{mech} + \varepsilon_{thermal}. \quad (1)$$

Stress is calculated from mechanical strain. If the value of thermal strain is higher than total strain, mechanical strain must be negative. Thermal strain in a point at the bottom surface of the slab depends on the temperature. Total strain is however given by the deformation of the structure, which is influenced by whole the structure. This phenomenon leads towards negative (compressive) stresses in places where normally not expected when not exposed to fire.

Convergences in approach #1 of geometry cases Ø8 and Ø6 are worse. To carry on with the analysis, approach #2 or even #3 needs to be applied. In general, the best convergences have been achieved by conducting the loading history in accordance with the approach #3.

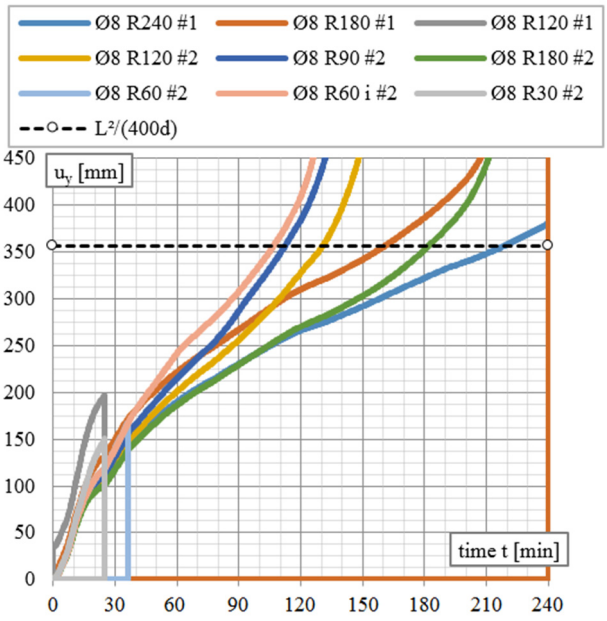

Fig. 7: Evolution of the mid-span deformation for Ø8 #1 and #2.

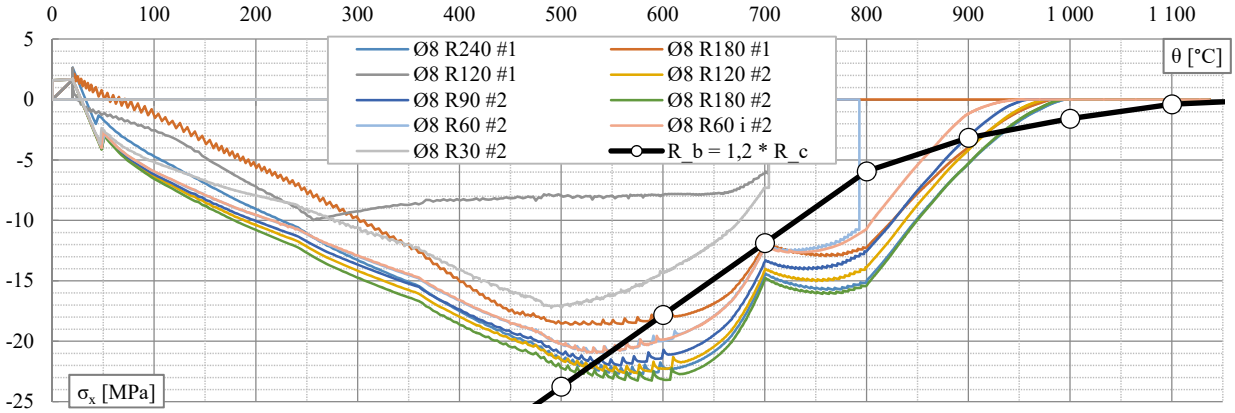

Fig. 8: Normal stress-in the mid-span of bottom (heated) surface in dependence on temperature.

Figure 8 depicts a dependence of the normal stress in the mid-span point of the bottom surface of the slab on the temperature of this point. Curious phenomena are being observed. Limit value of the biaxial compressive strength R_b is given by:

$$R_b = 1{,}2 \cdot R_c, \quad (2)$$

where R_c is a uniaxial compressive strength defined in dependence on the temperature according to [11]. Normally it is not expected that the compressive stress is at any point of the analysis higher than the compressive strength value. This was observed only in the bottom node(s) of the mesh. By a linear interpolation between temperatures at nodes of a bottom element, considering the stresses in upper and bottom nodes of this bottom element, it was found that this phenomenon occurs only at negligible height, and might be as a result of numerical calculations.

Certain oscillations are observed in the values of the stresses along the temperature (rising in time) in the transient analysis, even though damping was considered.

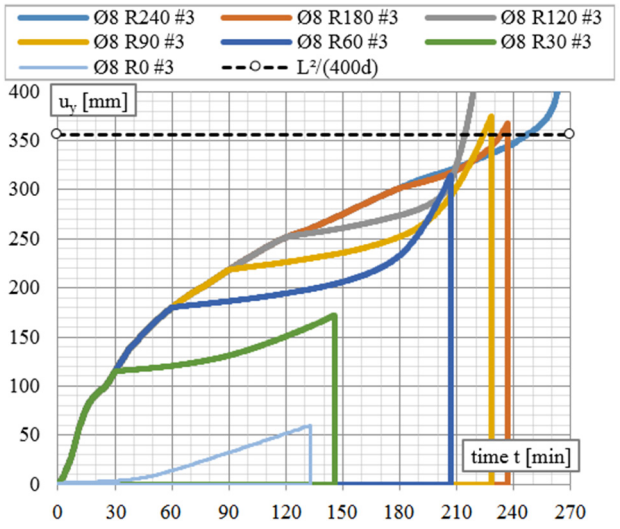

Fig. 9: Evolution of mid-span deformation in time for Ø8 #3.

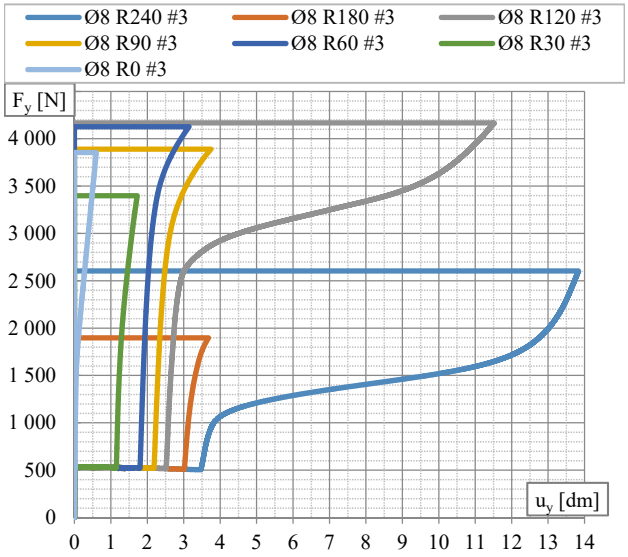

Fig. 10: Force mid-span deformation dependence.

When applying the mechanical load after the structure has been softened by the fire, it is feasible to demonstrate the Force-deformation curve, Fig. 10, and its numerical derivation, the bending stiffness curve, Fig. 11. The force F_y is a summarization of the total reactions in the vertical direction multiplied by 2, as the symmetrical half of the slab span has been modelled. Interesting phenomena is being observed in Fig. 11. The bending stiffness of slab in case R30 in time 90 min, therefore after 30 minutes of fire and 60 minutes of mechanical loading is at value of approx. 100 N/mm. In case R60 however, in time 120 min, therefore after 60 minutes of fire and 60 minutes of mechanical loading, the value of the bending stiffness is circa 155 N/mm. Similar in cases R90 and R120. The loading speed was the same for all the cases: 10 $kN \cdot m^{-2} \cdot hod^{-1}$. This seems to be an exception for the first case of R30, as the other cases compared with each other does not follow this pattern. For a final conclusion in this matter, more precise analysis would be required. The reason of local negative stiffness before the initiation of the mechanical loading (R30 and R60) is the decreasing density of concrete in dependence on the rising temperature.

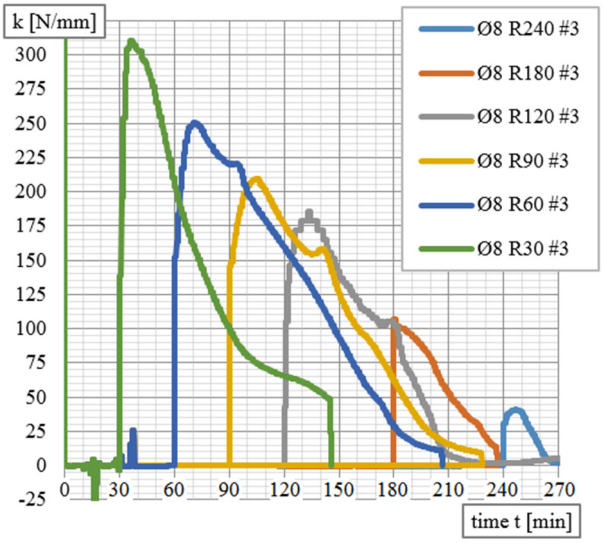

Fig. 11: Evolution of bending stiffness of the slab in time.

Problems with convergences in approach #1 and #2 of geometry case Ø6 were significant, and reasonable results have been achieved usually by the approach #3.

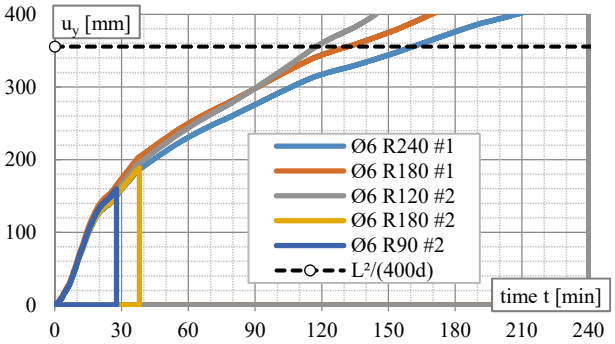

Fig. 12: Evolution of the mid-span deformation for Ø6 #1 and #2.

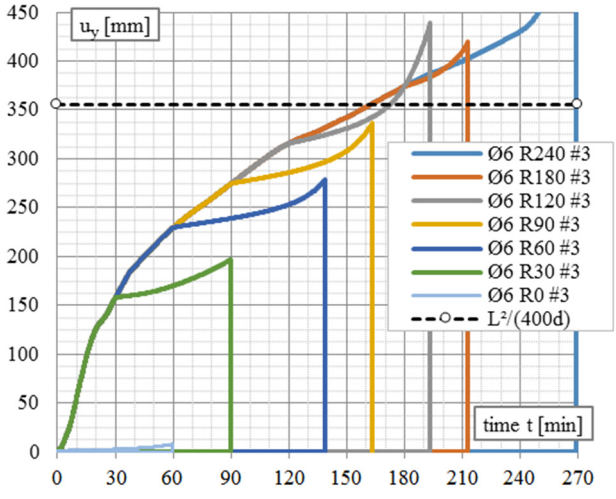

Fig. 13: Evolution of the mid-span deformation for Ø6 #3.

5. Discussion

A nonlinear FEM analysis of the concrete structure subjected to standard ISO 834 fire has been conducted. Software ANSYS was used to determine thermal and mechanical response of the structure. Simply supported reinforced concrete slab has been analysed. The results of mechanical fire resistance (based on limit mid-span deformation) have been compared with the expected values according to [11] in the manner described in the chapter 2. Results are summarized in the tables Tab. 1, to Tab. 4 below.

Tab.1: Summarization and comparison of results for Ø12 #1.

Ø12 #1	q [kN/m²]	time t [min]		(%)
		iso.500 °C	analysis	
R30	39.5	30	20.0	67
R60	33.0	60	110.0	183
R90	28.0	90	136.7	152
R120	25.0	120	150.0	125
R180	16.0	180	191.7	106
R240	9.0	240	240.0	100

Tab.2: Summarization and comparison of results for Ø8 #1 and #2.

Ø8	q [kN/m²]	time t [min]		(%)
		iso.500 °C	analysis	
R30 #2	18.0	30	25.0	83
R60 #2	17.0	60	106.7	178
R90 #2	17.0	90	110.0	122
R120 #2	14.5	120	130.0	108
R180 #1	7.0	180	160.0	89
R180 #2	7.0	180	180.0	100
R240 #1	2.0	240	220.0	92

Tab.3: Summarization and comparison of results for Ø8#3.

Ø8 #3	time t [min]		q [kN/m²]		(%)
	total	of app. q	iso.500 °C	analysis	
R0	133.3	133.3	19.0	22.2	117
R30	145.0	115.0	18.0	19.2	106
R60	205.0	145.0	17.0	24.2	142
R90	220.0	130.0	17.0	21.7	127
R120	215.0	95.0	14.5	15.8	109
R180	233.3	53.3	7.0	8.9	127
R240	246.7	6.7	2.0	1.1	56

Tab.4: Summarization and comparison of results for Ø6#3.

Ø6 #3	time t [min]		q [kN/m²]		(%)
	total	of app. q	iso.500 °C	analysis	
R0	60.0	60.0	9.5	10.0	105
R30	90.0	60.0	9.4	10.0	106
R60	138.3	78.3	9.4	13.1	139
R90	161.7	71.7	8.0	11.9	149
R120	171.7	51.7	6.7	8.6	129
R180	165.0	- 15.0	2.4	-2.5	x
R240	165.0	- 75.0	0.0	-12.5	x

Approach #1 seems to work well in cases of geometries where higher density of reinforcement has been applied (Ø12) and for higher (longer) resistance classes R (therefore less mechanical load applied). However, there are certain problems with convergence in case more practically reinforced concrete slab (geometry Ø8) is being analysed. Decreasing the time step integration during analysis is not always helpful. Finer meshes have not been analysed. It is possible that better convergence could be also achieved in case of approach #1 with finer mesh. However, this has not been studied in this work. Instead different approaches towards loading histories have been analysed. Approach #1 is chronologically correct one, where the fire load is applied after mechanical load. In the approach #2, these loads are applied simultaneously, and in reverse loading #3 the mechanical load is applied after the structure has been subjected to fire. Closer description is in chapter 2 of this paper.

For analysed geometries Ø8 and Ø6, approaches #2 and #3 have led towards better convergences. Usually the structure behaved more rigidly in approach #2 and the most rigidly in #3. See example in Fig. 14 and Tab. 5.

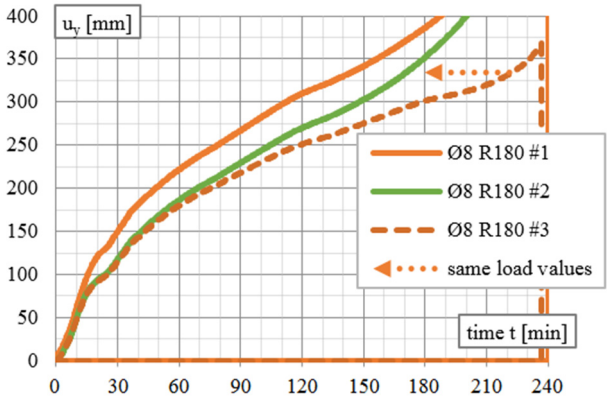

Fig. 14: Comparison of mid-span deformation evolutions for 3 different approaches of loading histories for geometry Ø8, class R180.

Tab.5: Detailed legend of loading histories for cases depicted in Fig. 14.

case	u_y (t_i) [mm]	t_i [min]	Applied loads in time (g = self-weight)		
			1 s	180 min	222 min
Ø8 R180 #1	386	180	g + 7 kN/m²	g + 7kN/m² + fire 180 min	g + 7 kN/m² + fire 222 min
Ø8 R180 #2	352	180	g	g + 7kN/m² + fire 180 min	g + 7 kN/m² + fire 222 min
Ø8 R180 #3	334	222	g	g + fire 180 min	g + fire 180 min + 7 kN/m²

6. Conclusion

Based on the experience and results of analysis, the following conclusions can be made:

- FEM software ANSYS can be used to evaluate the response of reinforced concrete structures exposed to fire load, taking into account nonlinear thermal and mechanical temperature-dependent properties of concrete and steel reinforcement.
- Definition of temperature-dependent parameters of nonlinear Menetrey-Willam material model for concrete is easily applicable, and the results of the analysis globally meets the expected values according to isotherm 500 °C method [11].
- Different loading history approaches during non-

linear analysis lead towards to different softening of the initial structure stiffness and therefore different results in calculation convergences. For analysed structure, the best convergences have been achieved while applying the mechanical load after the structure has been softened by fire, #3.

Acknowledgements

This paper has been created with the financial support of the project FAST-J-19-6030 provided by the Brno University of Technology fund for specific university research.

The authors would like to thank Faculty of Civil Engineering at Brno University of Technology, for the licence of the ANSYS product.

References

[1] DING, J. and Y. C. WANG. Realistic modelling of thermal and structural behaviour of unprotected concrete filled tubular columns in fire. *Journal of Constructional Steel Research*. 2008, vol. 64, iss. 10, p. 1086-1102. ISSN 0143-974X. DOI: 10.1016/j.jcsr.2007.09.014.

[2] DWAIKAT, M. and V. KODUR. Response of restrained concrete beams under design fire exposure. *Journal of Structural Engineering*. 2009, vol. 135, iss. 11, p. 1408-1417. DOI: 10.1061/(ASCE)ST.1943-541X.0000058.

[3] DWAIKAT, M. and V. KODUR. A simplified approach for predicting temperatures in fire exposed steel members. *Fire Safety Journal*. 2013, vol. 55, p. 87-96. ISSN 0379-7112. DOI: 10.1016/j.firesaf.2012.10.018.

[4] HAWILEH, R. and M. NASER. Thermal-Stress analysis of RC beams reinforced with GFRP bars. *Composites Part B*. 2012, vol. 43, iss. 5, p. 2135-2142. ISSN 1359-8368, DOI: 10.1016/j.compositesb.2012.03.004.

[5] HAWILEH, R., M. NASER, W. ZAIDAN and H. RASHEED. Modelling of insulated CFPR-strengthened reinforced concrete T-beam exposed to fire. *Engineering Structures*. 2009, vol. 31, iss. 13, p. 3072-3079. ISSN 0141-0296. DOI: 10.1016/j.engstruct.2009.08.008.

[6] KODUR, V., M. NASER, P. PAKALA and A. VARMA. Modelling the response of composite beam-slab assemblies exposed to fire. *Journal of Constructional Steel Research*. 2013, vol. 80, p. 163-173. ISSN 0143-974X. DOI: 10.1016/j.jcsr.2012.09.005.

[7] ZHOU, C. and F. VECCHIO. Nonlinear finite element analysis of reinforced concrete structures subjected to transient thermal loads. *Computers and Concrete*. 2005, vol. 2, iss. 6, p. 455-479. ISSN 1598-818X. DOI: 10.12989/cac.2005.2.6.455.

[8] DŽOLEV, I., M. CVETKOVSKA, Đ. LAĐINOVIĆ and V. RADONJANIN. Numerical analysis on the behaviour of reinforced concrete frame structures in fire. *Computers and Concrete*. 2018, vol. 21, iss. 6, p. 637-647. ISSN 1598-818X. DOI: 10.12989/cac.2018.21.6.637.

[9] ANSYS Inc. *ANSYS® Academic Teaching Mechanical: ANSYS Help Documentation*. Release 16.0, Canonsburg, 2017.

[10] DYNARDO GmbH. *MultiPlas: USER'S MANUAL.* MultiPlas 5.5.0, Weimar,2016.

[11] CSN EN 1992-1-2. *Eurocode 2: Design of concrete structures - Part 1-2: General rules - Structural fire design*. Prague: Czech Standards Institute, November 2006.

[12] CSN EN 1991-1-2. *Eurocode 1: Actions on structures - Part 1-2: General actions - Actions on structures exposed to fire*. Prague: Czech Standards Institute, 2004.

[13] CSN EN 1363-1. *Fire resistance tests - Part 1: General requirements.* Prague: ÚNMZ 2013.

[14] TORELLI, G., P. MANDAL, M. GILLIE and V. TRAN. A confinement-dependent load-induced thermal strain constitutive model for concrete subjected to temperatures up to 500 °C. *International Journal of Mechanical Sciences.* 2018, vol. 144, p. 887-896. ISSN 0020-7403. DOI: 10.1016/j.ijmecsci.2017.12.054.

[15] GAO, W., J. DAI, J. TENG and G. CHEN. Finite element modelling of reinforced concrete beams exposed to fire. *Engineering Structures*. 2013, vol. 52, p. 488-501. ISSN 0141-0296. DOI: 10.1016/j.engstruct.2013.03.017.

[16] KLINGSCH, E. *Explosive spalling of concrete in fire*. ETH Zűrich, Switzerland, 2014. Ph.D. Dissertation. Institut fűr Baustatik und Konstruktion.

[17] KUPILÍK, V. *Stavební konstrukce z požárního hlediska*. Praha: GRADA, 2006. ISBN 80-247-1329-2. (in Czech)